The SST-1M Telescope Camera in the TAIGA Observatory
Камера телескопа SST-1M в составе обсерватории TAIGA

M. Heller[a] [1], *A.N. Borodin*[b], *F. Cadoux*[a], *A.N. Demenko*[b], *V.M. Grebenyuk*[b,c], *O.A. Gress*[b,d], *A.A. Grinyuk*[b], *N. Kirichkov*[b], *M.V Lavrova*[b], *T. Montaruli*[a], *A. Nagai*[a], *A. Pan*[b,e], *A. Porelli*[b,f], *Y. Sagan*[b,c], *I. Satyshev*[b,e], *L.G. Tkachev*[b,c], *R. Wischnewski*[b,f], *D.P. Zhurov*[b,d,g]

[a] Départment de physique nucléaire et corpusculaire, Faculté de Sciences, Université de Genève, 24 Quai E. Ansermet, CH-1211, Switzerland

[b] Joint Institute for Nuclear Research, 141980, Dubna, Russia

[c] Dubna State University, 141980, Dubna, Russia

[d] Institute of Applied Physics, ISU, 664003, Irkutsk, Russia

[e] Institute of Nuclear Physics, Almaty, 050032, Kazakhstan

[f] Deutsches Elektronen-Synchrotron (DESY), D-15738 Zeuthen, Germany

[g] Irkutsk National Research Technical University, INRTU, 664074, Irkutsk, Russia

Гамма-обсерватория TAIGA комбинирует массив широкоугольных черенковских детекторов и атмосферные черенковские телескопы IACT (Imaging Atmospheric Cherenkov Telescopes), что обеспечивает более экономичный способ построения инструментов большой площади для гамма-астрономии свыше 10 ТэВ. В Тункинской долине строется прототип площадью ~ 1 км^2.

Планируется использовать камеру SST-1M, изначально разработанную для обсерватории CTA, для работы в 2020/2021 сезоне наблюдений как часть установки TAIGA. Эта основанная на кремниевых фотоумножителях камера с полностью цифровой системой считывания сигнала с частотой оцифровки 250 MHz и точной калибровкой предоставляет превосходную дополнительную информацию о ливне. Это позволит провести детальную калибровку с использованием, например, Крабовидной туманности в широком диапазоне энергий.

The TAIGA observatory combines a wide angle Cherenkov timing array and Imaging Atmospheric Cherenkov Telescopes (IACTs) as a cost-efficient way to build a large area instrument for gamma astronomy above 10 TeV. A 1 km^2 prototype is in construction in the Tunka valley, Siberia.

We plan to operate the SST-1M camera, originally developed for the CTA-Observatory, for the 2020/2021 observation season as part of TAIGA. This SiPM based camera features a fully digital 250 MHz waveform readout and precision calibration, and provides excellent complementary shower information. It will allow for detailed calibration using e.g. the Crab Nebula over a wide range of energies.

PACS: 44.25.+f; 44.90.+c

[1] E-mail: matthieu.heller@unige.ch

1. Introduction

Ground based high-energy gamma astronomy is a successful way to investigate galactic and extra-galactic sources of high-energy cosmic rays, their location and intrinsic acceleration mechanisms. Efforts are directed to significantly enlarge instrumented areas to multi-km^2 range, to boost detection sensitivities for energies beyond several TeV's.

A conceptually new approach to gamma ray detection beyond few 10 TeV is being developed by the TAIGA observatory (Tunka Advanced Instrument for cosmic ray physics and Gamma Astronomy). TAIGA builds a hybrid system of wide-angle timing and imaging Cherenkov detectors [1–3]. A 1 km^2 TAIGA prototype setup is currently being constructed in the Tunka valley, Siberia (50 km from Lake Baikal). Figure 1 gives an areal overview of the TAIGA setup, with its main components: the wide-angle non-imaging atmospheric Cherenkov stations of the timing array TAIGA-HiSCORE, the first IACT of the TAIGA-IACT array and the DAQ-center. In this new approach the reconstruction of the shower energy, location, and direction is performed using the timing array TAIGA-HiSCORE. To discriminate gamma rays from the hadron background, the IACTs are used. Each IACT can operate in mono-mode, the distances between telescopes can be at least up to 600 m, and possibly larger. This sparse instrumentation with IACTs, compared to stereo operation as e.g. foreseen in CTA, yields significant cost reduction when instrumenting large areas.

Fig. 1. Overview of the TAIGA Observatory. **Left**: Panoramic view with the array of TAIGA-HiSCORE stations and IACTs, and the DAQ-center. By early 2020, 1 km^2 of HiSCORE and three IACTs will be installed. Insert: a HiSCORE station and the IACT. **Right**: Schematic view of the HiSCORE array (∼100 stations, grouped in 4 color-indicated cluster) and the TAIGA-IACTs (red dots "1,2,3") and the new TAIGA-SST-1M location (red dot "4").

The TAIGA collaboration has developed the TAIGA-IACT, comprising a telescope with a 4.3 m reflector, a photomultiplier-based pixelized camera, and calibration and control systems; the first telescope is currently in commissioning at the TAIGA-site. At the same time, in the framework of the CTA-consortium, a variety of new telescopes and camera solutions for different energy ranges had been developed. The SST-1M Telescope was one of the proposed design to CTA for the gamma energy range between few TeV and few hundred TeV. It is based on the Davies-Cotton single mirror concept, and features a high-tech SiPM-based camera that allows full waveform recording of shower images at

250 MHz sampling rate, and was successfully evaluated at a test site.

This paper discusses science and technical aspects of operating the camera of the SST-1M telescope as part of the TAIGA observatory. In section 2 and 3, we review the main TAIGA components: TAIGA-HiSCORE and TAIGA-IACT. Section 4 highlights advantages and specifics of the SST-1M camera, and the chosen solution to integrate and operate it within the TAIGA observatory.

2. TAIGA-HiSCORE

Each station of the TAIGA-HiSCORE array comprises four photomultipliers (PMT) with a photocathode of 20 to 25 cm diameter (ET9352KB, R5912, or R7081) and the station data acquisition system (DAQ). Each PMT is equipped with a Winston cone made of a highly reflective material Alanod 4300 UD, which increases the effective light-collecting area by a factor of four, up to 0.5 m^2. The field of view (FoV) of the Winston cone is about 0.6 sr. The DAQ of TAIGA-HiSCORE has a hierarchical structure (Fig.2). The Cherenkov stations of the array are grouped in clusters of approximately 30 detectors

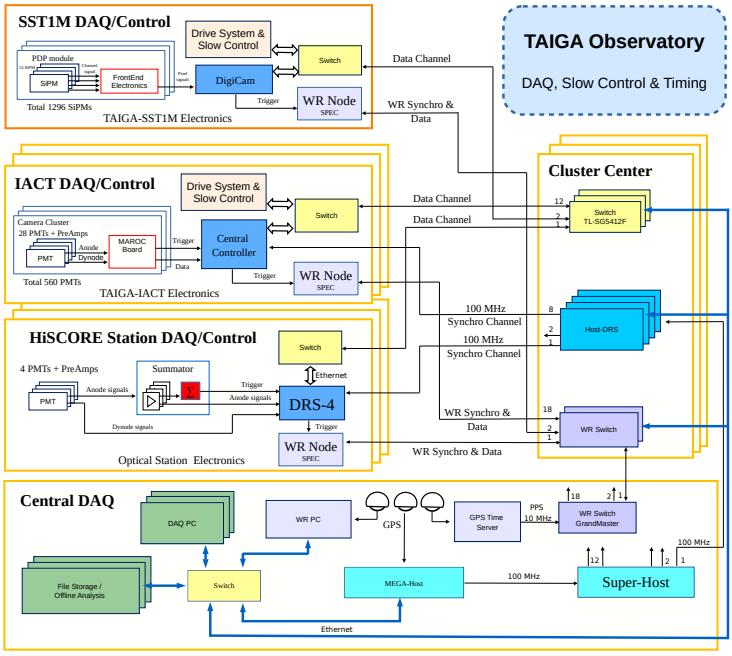

Fig. 2. The data acquisition, slow control and timing system, which comprises the Central DAQ (located in the central building), the Cluster centers (distributed over the field), and the DAQ components in HiSCORE-stations and IACTs. Indicated are Front-End components and both independent timing systems, as well as central servers and clocks. Also shown is the TAIGA-SST-1M telescope, integrated into the modular DAQ and the White Rabbit (WR)-timing system.

each. The main components of the Cherenkov station DAQ are analog summators and an 8-channel ADC based on the DRS-4 board, by means of which the signals from the anodes and the fifth dynode (to expand the dynamic range) of each PMT are digitized with a 0.5 ns step within a 200 ns window after the formation of the trigger. For moonless nights the trigger rate of a TAIGA-HiSCORE station is 10-15 Hz. All HiSCORE stations trigger independently; array-trigger or coincidences with the IACTs are selected offline.

The energy threshold of the array is 80-100 TeV for hadronic air showers and 40-50 TeV for showers initiated by gamma rays. Each HiSCORE station is connected to its Cluster Center by optical fibers, which serve for data transmission and synchronization. To reach best pointing precision of TAIGA-HiSCORE ($\sim$0.1 deg), a relative time synchronization between HiSCORE stations of sub-nsec precision is required [4, 5]. In addition, also IACT events should be time-stamped with a few nsec precision, to be included into the array pointing reconstruction. As indicated in Fig.2, two time-synchronization systems are operated in parallel, both receiving the same front-end trigger signals: a custom system using a 100 MHz clock distributed over optical fibers, and a White-Rabbit (WR) based system [1,5,6]. The latter is referencing to a precision GPS TimeServer (Meinberg Lantime M1000).

An important requirement for the TAIGA synchronization systems is their long-term stability. A precision cross comparison of stability of both systems is given in Fig. 3 [3]. The analysis uses the raw trigger times as obtained from both systems on an event-by-event basis, and compares the difference of time differences $\Delta t^{DAQ} - \Delta t^{WR}$ of trigger times, see Fig. 3 for details. The conclusion from this test is an excellent combined and individual stability performance of the two TAIGA timing systems: the rms of the differences of time-differences is < 0.7 ns, which implies a rms well below < 0.5 ns for each time-system independently.

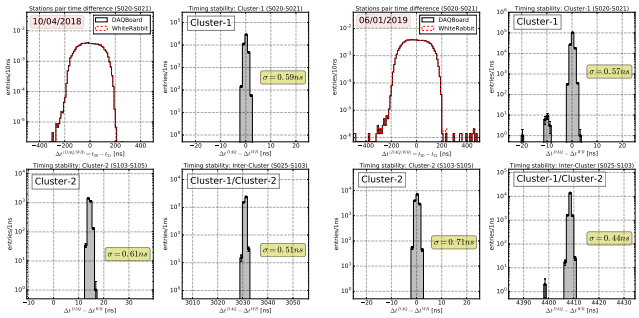

Fig. 3. Precision test of the two independent TAIGA timing systems, comparing the trigger timestamps on an event-by-event basis. Two days shown: **Left**: 10/04/2018, **Right**: 06/01/2019. (a) **Upper left**: time difference for two channels, as directly measured by the WR- and the 100 MHz systems ("DAQ"). (b) **Upper right**: difference of the times from (a) for each event, $\Delta t^{DAQ} - \Delta t^{WR}$. (c) **Lower left**: same as (b) for two channels from HiSCORE Cluster-2. (d) **Lower right**: same as (b) for two channels from HiSCORE Cluster-1 and Cluster-2.

3. TAIGA-IACT

The TAIGA telescope (Fig. 4) has an alt-azimuth mount and a camera in the focus of the segmented Davies-Cotton design reflector with 34 mirrors, each with a 0.6 m diameter and curvature radius of 9.5 m. The total diameter of the telescope reflector is 4.3 m, total mirror area is 9.6 m^2. The focal length of the telescope is 4.75 m where the telescope camera is installed. The TAIGA-IACT camera consists of a hexagonal grid of 560 XP1911 PMTs, each in a Winston cone and has a field of view of 9.6° (0.36° per pixel).

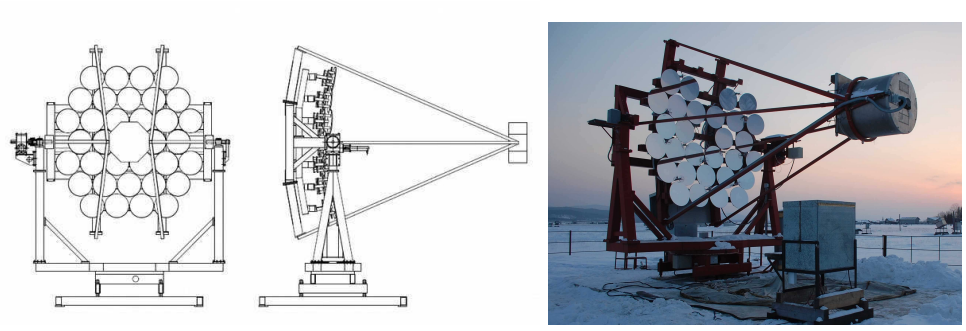

Fig. 4. The TAIGA-IACT telescope: sketch of the telescope (left) and the first TAIGA-IACT (right), operating in the TAIGA Observatory, Tunka valley, Siberia.

For telescope pointing calibration and measurements a CCD-camera Prosilica GC1380 is installed at a distance of ∼1 m from the telescope optical axis on the telescope dish near the mirror. The field of view of this camera is of 31.4° × 23.6° (0.023° per pixel). The CCD camera is located in such a position that its field of view allows capturing simultaneously on the same image the telescope camera and visible stars in the field of view of the telescope. Eight positioning LEDs are installed along the telescope camera perimeter to determine its position by the CCD images.

On each telescope axis, a hybrid stepper motor Phytron ZSH107/4.200.12,5 is installed in a heated box together with a system of two gearboxes. To perform readout of the axis position a 17-bit absolute shaft encoders is used. The motors, limit switches and shaft encoders are connected to the PhyMOTION control unit, which is connected to the DAQ center via Ethernet.

For the TAIGA-IACT pointing operation a pointing model is used. It is applied to the telescope shaft encoder data and intended to reduce pointing residuals, usually caused by a small telescope tilt, small non-perpendicularity of the telescope axes, telescope construction deformation caused by the gravity. Measurements for the pointing model calibration are performed using the CCD camera installed on the dish. To perform pointing measurements a white screen is installed in the telescope focus; this is also planned for the SST-1M camera.

During the tracking operation, the CCD camera is also used for control and monitoring of the telescope pointing direction. The astrometry.net software is used for the image astromery measurements. In order to transform CCD camera coordinates to the telescope camera focal plane coordinate system, the transformation described in [7] is used. In order to control the TAIGA-IACT telescope pointing calibration an additional

independent method is used. This method is based on measurements of the anode current on the central PMT during a special scan of a known bright star and by the profiles of the anode current the pointing error is determined. [3]. For the TAIGA-SST1M telescope similar measurements are in preparation and will be facilitated by the DC coupling of the electronics and the reguler monitoring of the baseline variations.

The TAIGA-IACT camera is divided into clusters, each consists of 28 PMTs and corresponding HV supply, and the readout electronics board. The cluster electronics is based on the 64-channel chip ASIC MAROC3. It provides signal processing and cluster trigger signals, as well as monitoring of PMT anode currents and count rates. Each MAROC channel features a preamplifier with adjustable gain factor, discriminator with adjustable threshold, integrating amplifier and 12-bit Wilkinson ADC. Each PMT signal is fed into 2 MAROC channels with different gain factors of the preamplifiers to extend the dynamic range up to ∼3000 p.e [8].

Camera trigger is based on the cluster hierarchy; a cluster trigger requires at least 3 (optionally 4 or 2) channels with signal amplitudes above ∼10 p.e. within 15 ns (high gain channels only). All clusters connect to the central control board, which produces the main camera trigger, sends data and synchronizes time with the DAQ center via optical fibers. Clusters are read out only if they have either produced a cluster-trigger, or have at least one pixel above the pixel threshold within a 160 ns coincidence window. This inherently limits a full readout of the image charge, and is under revision. Also, pixel signals with large time-separation (few 10 ns) from the event trigger time shift, will yield to distorted amplitude values (occurring for showers with large impact parameters).

An example of a joint hadron-like event, recorded by both TAIGA-HiSCORE and TAIGA-IACT, while the telescope was tracking the Crab Nebula, is shown in Fig. 5 [8]. For convenience, the EAS core position detected by HiSCORE is projected to the camera plane as asterisk with an additional scale factor: Rp (cm) / Rc (cm) = 1500, where Rp is the distance from the telescope to the EAS core position and Rc is the distance from the camera center to the asterisk. For events coming from the source to which the telescope is pointing, the line connecting the projection of the EAS axis and the center of gravity of the image should cross the camera center. Within the coincidence window of 2 μs

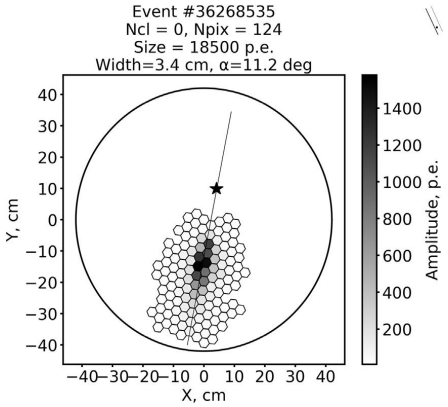

Fig. 5. An example of a TAIGA-IACT event, simultaneously detected and fully reconstructed also by TAIGA-HiSCORE.

the same event was detected with 15 stations by the TAIGA-HiSCORE array. It was reconstructed with following EAS parameters: E = 840 TeV, θ = 30.1°, ϕ = 33.6°, Rp =134 m, the angle between the direction of the shower and direction of the source is ψ = 0.47°. This nicely demonstrates the power of the hybrid detection of air showers by the non-imaging array and the IACT.

4. **The SST-1M Camera**

The SST-1M camera [9–11] has been developed by a consortium of Swiss and Polish institutes in the frame of the Cherenkov Telescope Array project (CTA). The SST-1M project [12] as a whole was one of the proposed designs for the small size telescopes array to equip the southern observatory of CTA. The project was eventually rejected but two prototype telescopes have been produced in the process.

The SST-1M telescope is based on a 4 m Davies-Cotton optics with a focal length of 5.6 m providing an f/D of 1.4. In this configuration, the angular pixel size is 0.24° and the total field of view 9°.

An exploded view of the SST-1M camera is shown in Fig. 6. Its main sub-systems are:

- an entrance window;
- a photo-detection plane;
- a fully digital trigger and readout electronics.

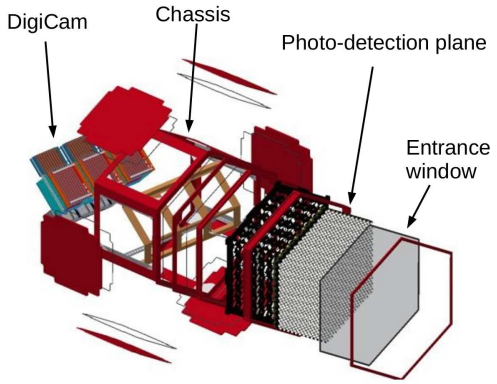

Fig. 6. CAD drawing of the SST-1M camera, exploded view.

The entrance window is made out of Borofloat33 and is 3.3 mm thick. An an anti-reflective coating together with a low-pass filter with a cut-off wavelength of 540 nm are applied on the substrate. These two coatings combined offer a better transmissivity in the near UV band and limits the night sky background contribution and therefore maximize the signal to noise ratio. The photo-detection plane has 1296 hexagonal pixels which are grouped 12 by 12 into 108 optical modules. Each pixel is composed of:

- a hollow light guide which a UV enhanced coating optimized for large incident angle;
- a hexagonal silicon photo-multiplier (SiPM) which results from the collaboration of the University of Geneva and Hamamatsu;
- a transimpedance amplifier, made out of discrete components, followed by differential amplifier;
- a bias voltage source which includes a compensation loop to account for temperature variations.

All pixels are connected to the digital readout system via standard Ethernet CAT6 cables conveying the differential signals. The digital readout, called DigiCam [13], features three mini-crates composed each of nine FADC boards and one trigger board. Each mini-crate digitizes the analog signals of one third of the camera at a sampling frequency of 250 MHz. One of the trigger boards in one mini-crate acts as a master and collects every 4 ns a compressed image of the camera. Based on this image, a trigger decision is taken if the signal collected in any group of 21 neighboring pixels exceeds a pre-defined threshold. In such case, the readout window of programmable length of the 1296 pixels is readout. This design uses ring-buffers which provide a dead time probability of 10^{-8} at a trigger rate of 600 Hz.

The SST-1M camera has been extensively calibrated in the laboratory and then tested on-site during two observation campaigns in the IFJ at Krakow, Poland. The laboratory measurements aimed at demonstrating that the camera was meeting the requirements imposed by the CTA Observatory. For instance, the linearity of the response was measured as function of the number of photo-electrons and is shown in Fig. 7–left. It demonstrates that the linearity is achieved up to $\sim$750 p.e. After this stage, the pre-amplifier chain is saturated and the linearity is lost. Nevertheless, using an adjustable integration window, it was demonstrated that a monotonic response is achieved which maintain the charge resolution within requirements even with a background of 600 MHz of p.e. per pixel (see Fig. 7–right).

The timing resolution of single pixel as a function of the number of true p.e., i.e. corrected for the optical cross-talk of the SiPM sensor is shown in Fig. 8. This result was obtained by emulating a background light rate of 125 MHz p.e. per pixel. It is shown that above 10 p.e., a time resolution better than 1 ns is reached. This performance are relevant for the combination with the TAIGA-HiSCORE stations.

Before each observation run, a dark run is acquired with the camera shutter closed. In these conditions, only the so-called thermal photo-electrons contributes to the detected signal. The distribution of the waveform raw ADC values can be used to monitor the pixel characteristics (e.g. gain, optical cross talk, dark count rate). Fig. 9 shows the stacked distributions of all camera pixels for all observation nights done in Krakow. The bumps are the different photo-electron contributions coming for the optical cross-talk. The fact that up to seven bumps can be observed denote the remarkable stability and uniformity of the pixel response. These data can be used to monitor the long term evolution of the sensor characteristics.

Fig. 10–left shows the rate of background light as measured during the observation of Crab nebulae in 2018 at Krakow as a function of the azimuth and elevation angles. The

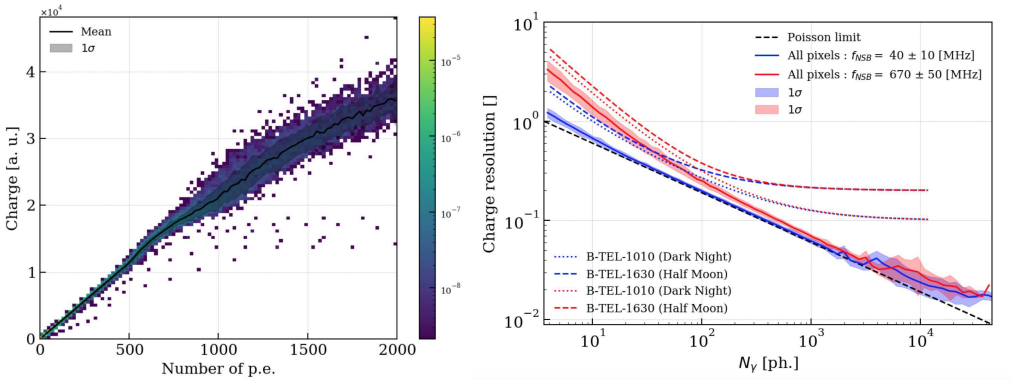

Fig. 7. Reconstructed charge as a function of the true number of photo-electrons (corrected for optical cross-talk) for all camera pixels of the SST-1M camera (left). Charge resolution as a function of the true number of photons for different night-sky background levels. The solid lines represent the average charge resolution of the camera and the contoured band its 1-sigma deviation among all camera pixels (right).

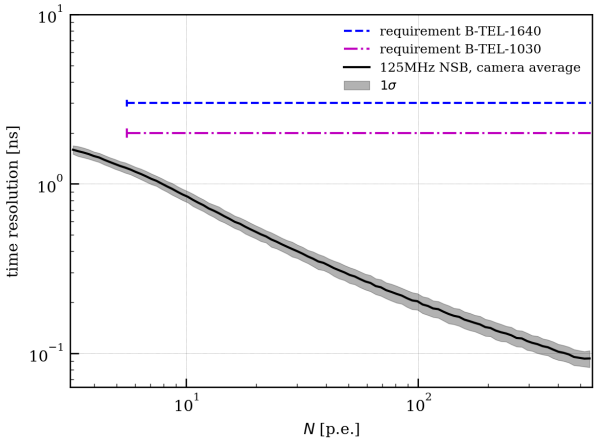

Fig. 8. Average time resolution for all pixels of the SST-1M camera as function of the number of photo-electrons for an average background light of 125 MHz of photo-electrons per pixel. The dotted lines indicate the performance requirements imposed by CTA.

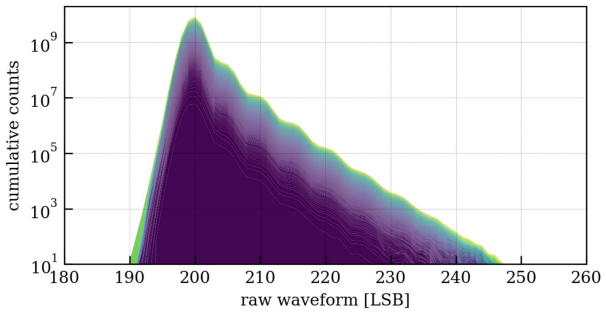

Fig. 9. Stacked distribution of the raw ADC waveforms for all pixels during all observation nights of the 2018 observation campaign in Krakow. The dotted lines indicate the performance requirements imposed by CTA.

poor quality of the site for astronomical observations can be seen as the background rate per pixel ranges from 0.4 to 1.4 GHz. But more importantly, it shows the capability of the SST-1M camera to exploit the DC-coupling of its electronics to measure the background light level and apply the relevant corrections for the image calibration. Fig. 10–right shows the trigger rate and the average night sky background rate (NSB) per pixel during one hour of observation in Krakow. The spikes observed in both curves are planes crossing the field of view of the telescope. One can see that the lower is the NSB rate, the higher is the trigger rate. This counter intuitive observation can be explained by the fact that a constant illumination induces a voltage drop across a resistor mounted in series with the bias circuitry of the sensor. This voltage drop translates into a gain, photo-detection efficiency and optical cross talk drop. This effect has been extensively studied and is part of the calibration chain of the SST-1M camera response [14].

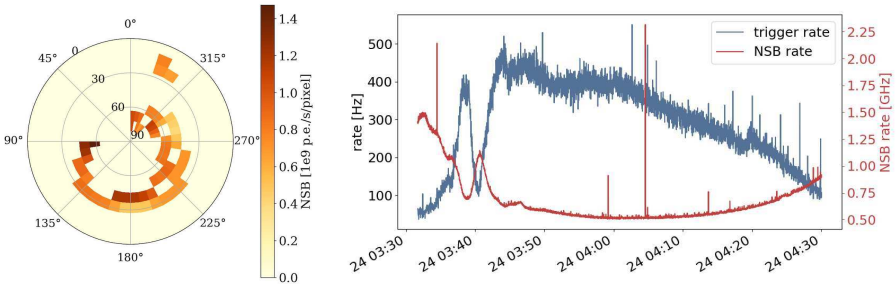

Fig. 10. Left: Average NSB value as a function of azimuth and elevation angle. Right: Evolution of the NSB and trigger rate as a function of the time for a typical observation run.

Given the focal length of the TAIGA-IACT telescope, the angular pixel size of the SST-1M will be 0.28° for a total field of view of 10.1°.

A dedicated mechanical interface will be developed to adapt mount the SST-1M camera to the current TAIGA-IACT telescope structure. Because the SST-1M camera is very close in size to the current camera and therefore, the mechanical interface will

be very similar to the existing one and will be developed by the Design Department of DLNP, JINR.

A conceptual CAD drawing can be seen in Fig. 11 with a prototype interface. In order to ease the adaptation to the environmental conditions, it is also foreseen to fit the SST-1M camera into a sealed cylinder as it is currently done with the existing camera. That would allow to add heaters in the cylinder and limit the temperature gradient at the camera–wall interface.

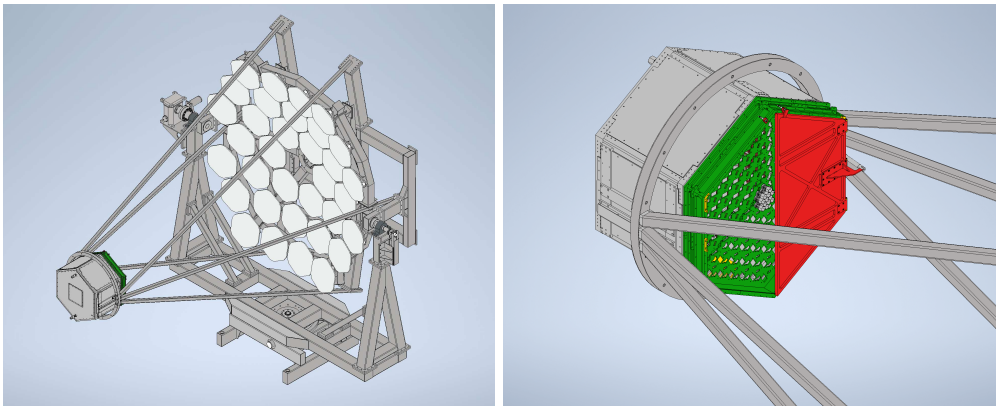

Fig. 11. CAD view of the SST-1M camera mounted to on the TAIGA telescope (left). Zoomed view, with lid partially opened (right).

The other major aspects to consider in order to operate safely the SST-1M camera are the environmental conditions of the Tunka site and in particular the very low temperatures. The measurements done on-site are summarized in Fig. 12. These graphs show that in winter, the daily average temperature can reach -40°C for which the SST-1M camera has not been designed for. This temperature is indeed very close to the minimal storage temperature of every component of the camera. A closer look on the required thermal operation conditions is given in Fig. 13. It shows the fraction of useable observation time (selecting only dark nights from the 2-year dataset in fig. 12), that is obtained for different camera operation conditions T_{min}, T_{max}, i.e. assuming the camera is operating for temperatures $T > T_{min}$ and $T < T_{max}$. For $T_{min} = -39°\mathrm{C}$ observation time losses are kept below 5% for the long dark winter nights. The upper limit T_{max} is less critical, $T_{max} = 16°\mathrm{C}$ is an acceptable value.

This observation imposes the modification of the environmental control of the camera and its cooling system. Concerning the environmental control, heaters have to be installed inside the camera housing to maintain an acceptable temperature ($> 0°\mathrm{C}$) at all time. The current wiring scheme allow for extra 1.5 kW dedicated for the heating. It was therefore decided that three air pulsed heaters of 400 W each will be installed in the camera in order to evenly distribute the heat between the photo-detection plane and the rest of the camera housing. Compared to this rather simple modification, the revision of the cooling design requires more studies and has not been finalized yet. The current SST-1M design uses water cooling in order to efficiently extract heat from all heating components (photo-detection plane and digital readout electronics). On the SST-1M

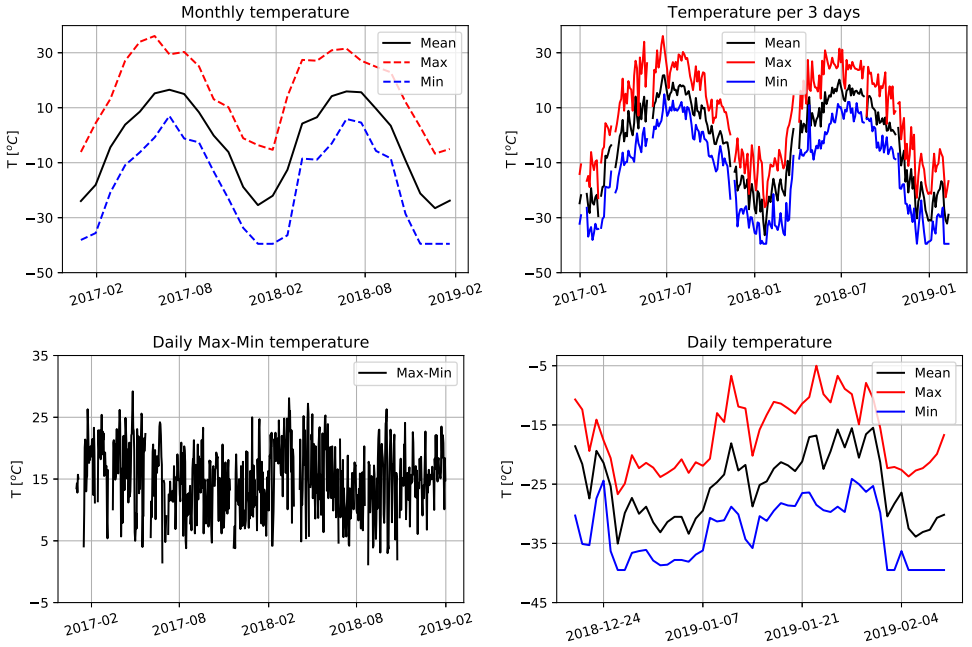

Fig. 12. Temperatures measured at the Tunka site from January 2017 to February 2019. Mean, maximum and minimum temperatures per month (top-left), for three days (top-right) and per day for the 2018/2019 winter (bottom-right) are plotted against the date. The difference between the maximum and minimum daily temperature as function of date is shown on the bottom-left.

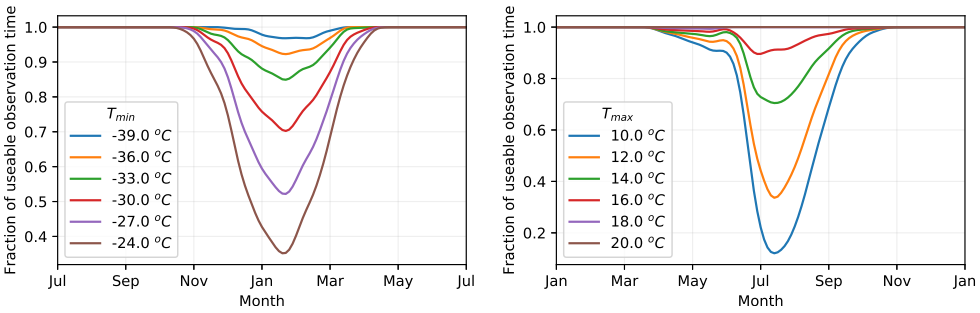

Fig. 13. Fraction of usable observation time (dark, moonless time) for different seasons under the assumption that the camera is operating for temperatures $T_{min} < T$ (left) and $T < T_{max}$ (right).

telescope, a chiller with a 0.4 MPa pump is used to push the water from a dedicated cabinet to the camera. A total of 52 m of water pipes is needed to do so. With this pipe length, a flow of about 8 l/min for 80/20% water/glycol coolant mix is reached. However in order to sustain temperatures down to -40°C, the coolant must be at least 48/52% water/glycol. In this proportions, at 0°C, the fluid would have a 20% lower specific heat, and thermal conductivity and a three times higher dynamic and cinematic viscosity. With such conditions, it would be impossible to reach a flow of 8 l/min and in addition, regardless of the flow, the coolant would be about 20% less efficient to extract the heat of the camera($\sim$1.8 kW).

Consequently an alternative cooling system has to be developed to overcome these limitations. Several technical solutions have been envisaged:

- passive systems:
  - heat pipes coupled to heatsinks mounted on the external part of camera housing
- active systems:
  - Peltier elements coupled to heat pipes that guide the heat to heatsinks mounted on the external part of camera housing
  - water/glycol based cooling with increased pipe diameter
  - water/glycol based cooling mounted at the back of the camera

The solutions using heat pipes have been discarded due to their complexity and the significant modifications that would be required to implement them. Concerning the water/glycol based cooling solutions, both are being studied. In both cases, the use of a commercial chiller is not considered as it would require to build a environmentally controlled cabinet around which would add an unnecessary level of complexity. A simpler system using a pump and radiators for the heat transfer will be designed. Given the low temperatures, forced convection should provide the required heat dissipation. Tests inside a climate chamber will be performed in 2020 to validate the proposed design.

Work regarding integration of SST-1M into the TAIGA-DAQ system has started. The TAIGA timing system has a modular design, which makes it straightforward to integrate the SST-1m camera trigger time-stamping. Each camera trigger will be time-stamped with nsec-precision by a White-Rabbit (WR) node located in the SST-1M camera [5,15], as indicated in Fig. 2. These trigger messages are delivered to the central counting house. An update of WR-nodes performance to >10 kHz high-speed is in preparation. At the same time, the WR-node can deliver precision clock signals (1 PPS and 10 MHz) directly to the SST-1M camera.

Camera science data transfer to the DAQ-center will be over 1 or 10 Gbps network fiber connection from the SST-1M Camera through the local cluster center (see Fig. 2).

The SST-1M configuration for the Monte-Carlo simulation package sim_telarray [10, 11, 16] will be used to study standalone as well as combined with HiSCORE operation of the STT-1M camera. In addition, an adaptation of the dedicated TAIGA IACT/HiSCORE MC will be used for cross-checks [17].

As the software for the TAIGA-IACT (drive, CCD-camera) and SST-1M camera were developed using different frameworks (the EPICS and the ALMA Common Software) for intercommunication between these systems an adaptation software will be developed. The existing OPC-UA layer developed for the SST-1M slow-control can be used as starting point to integrate it to the EPICS framework. The TAIGA-IACT pointing data processing pipeline will be adapted for the digicampipe[1] software, that is based on the ctapipe[2] data analysis framework and is developed for the SST-1M camera data processing. At a later stage of the analysis chain, the TAIGA-HiSCORE data will be added to the processing pipe to perform a hybrid analysis.

5. Conclusions

The TAIGA Observatory is under construction in the Tunka valley, Siberia (Russia). TAIGA follows an innovative concept for ground based gamma astronomy beyond 10 TeV - it operates an array of non-imaging wide-aperture atmospheric Cherenkov stations (HiSCORE) in conjunction with a few Imaging Air Cherenkov Telescopes (IACTs). The TAIGA prototype will reach an instrumented area of 1 km^2 with $\sim$100 stations, and three IACTs (the first is currently in commissioning), with an expected point source sensitivity of 2.5×10^{-13} TeV cm^{-2} sec^{-1} (for 300 hr observation).

Here, we outline the operation of the SiPM-based SST-1M camera with 250 MHz waveform readout and fully digital trigger, originally developed for the Cherenkov Telescope Array (CTA), as part of the TAIGA Observatory. The TAIGA-SST-1M telescope is well suited for precision detection of gamma induced showers of highest energies and large distances with increased duty cycle; it will significantly contribute to the TAIGA calibration by e.g. observing the Crab Nebula - both in standalone operation (above few TeV) as well as in full hybrid operation mode (above few 10 TeV's), and will increase the sensitivity to galactic and extra-galactic gamma sources.

Acknowledgements

This work is supported by the Russian Science Foundation, under grant 19-72-20173. We acknowledge support by the European Union's Horizon 2020 program (Grant No 653477). We greatly acknowledge financial support from the Swiss State Secretariat for Education, Research and Innovation SERI. The SST-1M cameras have originally be developed for use in CTA by a consortium comprising the University of Geneva (coordinator), a Polish Consortium and a Czech Consortium of Institutes. They have been financed, with associated work, by the Swiss National Foundation SNF, by the University of Geneva Boninchi Foundation and by the State Secretariat for Education, Research and Innovation SERI ([www.sbfi.admin.ch]). The test work done for TAIGA is financed by the University of Geneva.

[1] https://github.com/cta-sst-1m/digicampipe
[2] https://github.com/cta-observatory/ctapipe

REFERENCES

1. *Budnev N. et al.* [TAIGA Collaboration] The TAIGA experiment - a hybrid detector for very high energy gamma-ray astronomy and cosmic ray physics in the Tunka valley // Poceedings of Science PoS(ICRC2017)768. — 2017. — V. 301. — P. 768. — URL: https://pos.sissa.it/301/768/pdf.

2. *Kuzmichev L. et al.* [TAIGA Collaboration] Tunka Advanced Instrument for cosmic rays and Gamma Astronomy (TAIGA): Status, results and perspectives // EPJ Web of Conferences. — 2017. — jun. — V. 145. — P. 01001. — URL: http://www.epj-conferences.org/10.1051/epjconf/201714501001.

3. *Budnev N. et al.* [TAIGA Collaboration] TAIGA—A hybrid array for high-energy gamma astronomy and cosmic-ray physics // Nuclear Instruments and Methods in Physics Research, Section A: Accelerators, Spectrometers, Detectors and Associated Equipment. — 2019. — URL: https://doi.org/10.1016/j.nima.2019.04.067

4. *Hampf D., Tluczykont M., Horns D.* Event reconstruction techniques for the wide-angle air Cherenkov detector HiSCORE // Nuclear Instruments and Methods in Physics Research, Section A: Accelerators, Spectrometers, Detectors and Associated Equipment. — 2013. — V. 712. — P. 137–146. — arXiv:1302.3957.

5. *Porelli A. et al.* [TAIGA Collaboration] Timing calibration and directional reconstruction for Tunka-HiSCORE // Journal of Physics: Conference Series. — 2015. — aug. — V. 632, no. 1. — P. 012041. — URL: http://stacks.iop.org/1742-6596/632/i=1/a=012041?key=crossref.e1065aaaae2955596de36bb4380e66ad.

6. *Gress O. et al.* [TAIGA Collaboration] The wide-aperture gamma-ray telescope TAIGA-HiSCORE in the Tunka Valley: Design, composition and commissioning // Nuclear Instruments and Methods in Physics Research, Section A: Accelerators, Spectrometers, Detectors and Associated Equipment. — 2017. — feb. — V. 845. — P. 367–372. — URL: https://www.sciencedirect.com/science/article/pii/S016890021630849X.

7. *Zhurov D. et al.* [TAIGA Collaboration] First results of the tracking system calibration of the TAIGA-IACT telescope // Journal of Physics: Conference Series. — 2019. — feb. — V. 1181. — P. 012045. — URL: https://doi.org/10.1088/1742-6596/1181/1/012045.

8. *Lubsandorzhiev N. et al.* [TAIGA Collaboration] The hybrid installation TAIGA: design, status and preliminary results // Poceedings of Science PoS(ICRC2019)729. — 2019. — V. 358. — P. 729. — URL: https://pos.sissa.it/358/729/pdf.

9. *Schioppa E.J. et al.* [CTA SST-1M Project Collaboration] The SST-1M camera for the Cherenkov Telescope Array // Proceedings of Science. — 2015. — aug. — V. 30-July-20. — arXiv:1508.06453.

10. *Al Samarai I. et al.* [CTA SST-1M Project Collaboration] Performance of a small size telescope (SST-1M) camera for gamma-ray astronomy with the Cherenkov Telescope Array // Poceedings of Science PoS(ICRC2017)758. — 2017. — aug. — V. 301. — P. 758. — arXiv:1709.03914.

11. *Jurysek J. et al.* [CTA Consortium Collaboration] Monte Carlo study of a single SST-1M prototype for the Cherenkov Telescope Array // Poceedings of Science PoS(ICRC2019)708. — 2019. — jul. — V. 358. — P. 708. — arXiv:1907.08061.

12. *Heller M. et al.*. An innovative silicon photomultiplier digitizing camera for gamma-ray astronomy // The European Physical Journal C. — 2017. — jan. — V. 77, no. 1. — P. 47. — arXiv:1607.03412.

13. *Rajda P. et al.*. DigiCam - Fully digital compact read-out and trigger electronics for the SST-1M telescope proposed for the cherenkov telescope array // Poceedings of Science PoS(ICRC2015)931. — 2015. — V. 236. — P. 931. — arXiv:1508.06082.

14. *Nagai A., Alispach C., della Volpe D., Heller M., Montaruli T., Njoh S., Reniera Y., Troyano-Pujadas I.* SiPM behaviour under continuous light. — 2019. — arXiv:1910.00348.

15. *Wischnewski R., Brueckner M., Porelli A.* Time Synchronization with White Rabbit - Experience from Tunka-HiSCORE // Poceedings of Science PoS(ICRC2015)1041. — V. 236. — 2015. — P. 1041. — URL: http://pos.sissa.it/236/1041/pdf.

16. *Moderski R. et al.* [CTA Consortium Collaboration] Performance of the SST-1M telescope of the Cherenkov Telescope Array observatory // Poceedings of Science PoS(ICRC2015)1008. — 2016. — V. 236. — P. 1008. — arXiv:1508.06459.

17. *Grinyuk A., Postnikov E., Sveshnikova L.* Monte Carlo simulation of the TAIGA hybrid gamma-ray experiment // Proc. of the 2nd International Symposium on Cosmic Rays and Astrophysics, ISCRA-2019. — 2019.